Neuron, Vol. 21, 593–606, September, 1998, Copyright ©1998 by Cell Press

CaMKIIβ Functions As an F-Actin Targeting Module that Localizes CaMKIIα/β Heterooligomers to Dendritic Spines

Kang Shen, Mary N. Teruel, Kala Subramanian, and Tobias Meyer*
Department of Cell Biology
Duke University Medical Center
Durham, North Carolina 27710

Summary

Ca^{2+}/calmodulin-dependent protein kinase II (CaMKII) is a serine/threonine protein kinase that regulates long-term potentiation and other forms of neuronal plasticity. Functional differences between the neuronal CaMKIIα and CaMKIIβ isoforms are not yet known. Here, we use green fluorescent protein–tagged (GFP-tagged) CaMKII isoforms and show that CaMKIIβ is bound to F-actin in dendritic spines and cell cortex while CaMKIIα is largely a cytosolic enzyme. When expressed together, the two isoforms form large heterooligomers, and a small fraction of CaMKIIβ is sufficient to dock the predominant CaMKIIα to the actin cytoskeleton. Thus, CaMKIIβ functions as a targeting module that localizes a much larger number of CaMKIIα isozymes to synaptic and cytoskeletal sites of action.

Introduction

Ca^{2+}/calmodulin-dependent protein kinase II (CaMKII) is a ubiquitous kinase that is expressed at high concentrations in neurons and at lower concentrations in most other cell types. Previous studies suggested that CaMKII is an essential mediator for long-term potentiation and other forms of synaptic plasticity (reviewed by Soderling, 1993; Braun and Schulman, 1995). Furthermore, CaMKII activity may have an important role in stabilizing the dendritic architecture (Wu and Cline, 1998). A critical neuronal function of the α isoform of CaMKII (CaMKIIα) was directly demonstrated by studying mice that were either lacking CaMKIIα or expressed mutated CaMKIIα. CaMKIIα-deficient mice as well as transgenic mice expressing an autonomously active or an autophosphorylation-deficient CaMKIIα showed impaired long-term potentiation as well as defects in spatial learning and memory (Silva et al., 1992; Chapman et al., 1995; Mayford et al., 1995, 1996; Glazewski et al., 1996; Gordon et al., 1996; Giese et al., 1998).

Since not only CaMKIIα but also CaMKIIβ is a prominent isoform in the central nervous system, the question arises whether CaMKIIα and CaMKIIβ have different roles in regulating neuronal functions. Such functional differences between the two isoforms would have a direct impact on our understanding of cell type–specific signaling processes, since the relative expression of CaMKIIα and CaMKIIβ is markedly different in different brain regions and at different developmental stages. For example, the ratios of α and β subunits are about 3:1 and 1:4 in adult forebrain and cerebellum, respectively, while in 10-day-old postnatal mice, the forebrain α:β ratio is 1:1 (Miller and Kennedy, 1985). On a structural basis, recombinant CaMKIIα as well as purified brain CaMKII has been shown to form oligomers with ~8 to 12 subunits (Bennett et al., 1983; Kanaseki et al., 1991). CaMKIIβ and CaMKIIα have a similar overall domain organization and corresponding autophosphorylation consensus sequences, and even though the calmodulin binding affinity of CaMKIIβ is slightly higher than that of CaMKIIα, the regulation of different CaMKII isoforms by Ca^{2+}/CaM and autophosphorylation is similar overall (Miller and Kennedy, 1985; GuptaRoy and Griffith, 1996; De Koninck and Schulman, 1998). Despite these similarities, it has been controversial whether CaMKIIβ forms oligomers on its own (Yamauchi et al., 1989), whether CaMKIIα and CaMKIIβ form heterooligomers when expressed at the same time (Kanaseki et al., 1991), and whether the two isoforms are differentially localized within cells (Scholz et al., 1988; Nomura et al., 1997).

Why is the homo- and heterooligomerization of CaMKIIα and CaMKIIβ important? Earlier studies have shown that oligomerization is required for physiological autophosphorylation of a threonine residue at position 286 in CaMKIIα (Hanson et al., 1994; Mukherji and Soderling, 1994). When autophosphorylated at this site (or at threonine 287 for CaMKIIβ), CaMKII is partially active in the absence of Ca^{2+}/CaM (autonomous activity) (Lai et al., 1986; Lou et al., 1986; Miller and Kennedy, 1986; Schworer et al., 1986) and exhibits a several hundred–fold increase in calmodulin binding affinity (trapping of calmodulin) (Meyer et al., 1992). In addition to this regulatory function, it is conceivable that oligomerization has a fundamental role in the localization of CaMKII. Since CaMKIIα is the predominant isoform in the brain, it can be hypothesized that the main function of CaMKIIβ isoforms is to indirectly alter the localization of CaMKIIα isoforms by first forming CaMKIIα/β heterooligomers and then localizing the mixed complex to new docking sites. Such a heterologous targeting mechanism would enable cells to alter the cellular localization of CaMKIIα indirectly by controlling the ratio of CaMKIIβ to CaMKIIα expression.

Here, we use green fluorescent protein–tagged (GFP-tagged) CaMKIIα and CaMKIIβ isoforms to explore the subcellular localization and oligomerization of CaMKIIα and CaMKIIβ. We found that dendritic spines and filopodia as well as the cortical cytoskeleton are the primary docking sites for expressed CaMKIIβ. In contrast, expressed CaMKIIα was uniformly distributed in the soma and processes and was largely absent from spines. However, when expressed in the same cell, CaMKIIβ targeted CaMKIIα to dendritic spines and the cell cortex. In vitro binding studies suggested that this targeting results from a direct binding interaction of CaMKIIβ with F-actin. We then developed a GFP-based protein–protein interaction assay ("Pull-Out" binding assay) to explore the binding interactions between CaMKIIα and CaMKIIβ isoforms in living cells. When expressed alone, CaMKIIβ was found to form homooligomers with an average size that is markedly smaller than the ~13 subunits measured for CaMKIIα homooligomers. When

*To whom correspondence should be addressed.

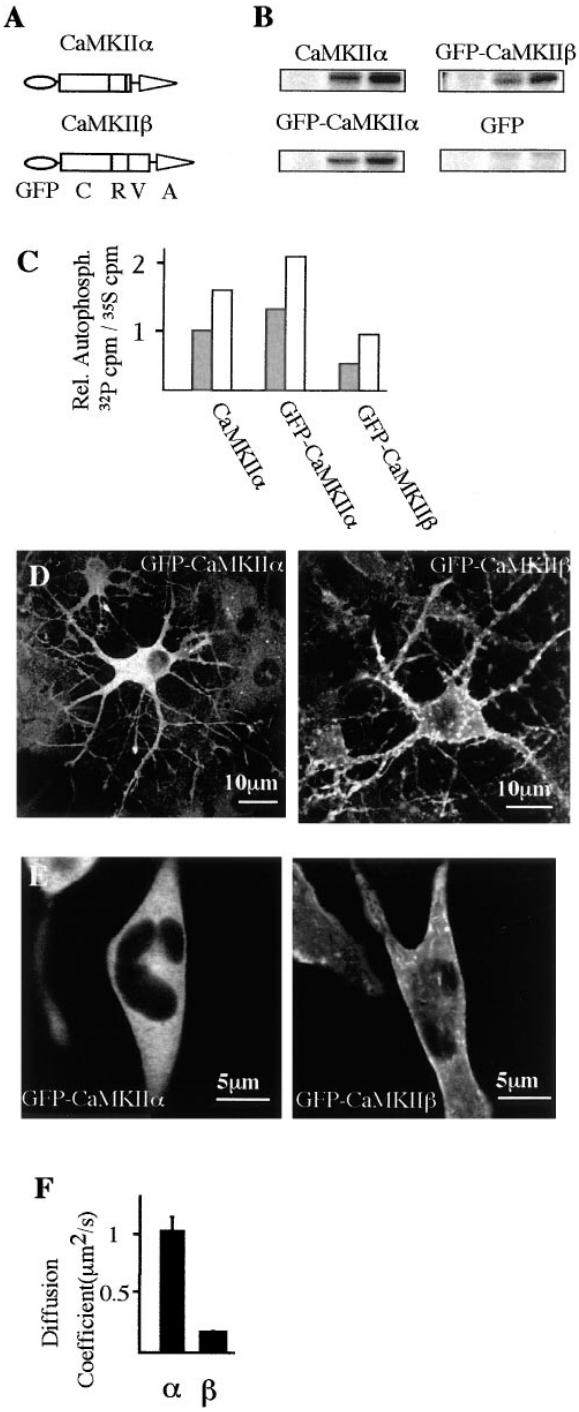

Figure 1. Cellular Localization and Mobility of GFP-Tagged CaMKIIα and CaMKIIβ

(A) Schematic representation of the domain organization of the GFP-tagged CaMKII isoforms. The catalytic domain (C), regulatory domain (R), variable domain (V), and oligomerization domain (A) are shown.

(B) Autophosphorylation of GFP-tagged CaMKII isoforms. Comparison of the baseline (left), calcium/CaM-dependent (middle), and burst (right) autophosphorylation activity of CaMKIIα, GFP–CaMKIIα, and GFP–CaMKIIβ. The kinase activity of the in vitro translated constructs are shown. Translated GFP alone was included as a control.

(C) Relative kinase activity corrected for the amount of expressed CaMKII or GFP–CaMKII protein (measured as the ratio of ^{32}P incorporation and $[^{35}S]$Met incorporation). The dark bars show CaMKII autophosphorylation after incubation with $[^{32}P]$ATP in high Ca^{2+}/CaM for 30 s. The light bars show the calcium-independent "burst" autophosphorylation after 30 s in high calcium and 120 s in EGTA.

(D) Confocal image of GFP-tagged CaMKIIα (left) and CaMKIIβ (right) expressed in living hippocampal CA1–CA3 neurons. Notice the homogeneous distribution of GFP–CaMKIIα throughout the soma and major branches, while CaMKIIβ is enriched in the dendritic branches.

(E) Confocal image of GFP-tagged CaMKIIα (left) and CaMKIIβ (right) expressed in living RBL cells. Notice the cortical staining and nonuniform internal staining of GFP–CaMKIIβ and the homogeneous distribution of GFP–CaMKIIα.

(F) Comparison of the calculated diffusion coefficients for GFP–CaMKIIα and GFP–CaMKIIβ.

expressed at the same time, CaMKIIβ isoforms incorporated equally well into either CaMKIIα or CaMKIIβ oligomers (and vice versa). Half-maximal targeting of CaMKIIα oligomers to the cytoskeleton was achieved if at least 15% of CaMKIIβ were present in the same cell, suggesting that a small number of CaMKIIβ subunits are required to dock CaMKIIα/β heterooligomers with ~13 subunits to F-actin. Our studies suggest that the synaptic localization of CaMKII activity is controlled by the relative expression of CaMKIIβ F-actin–docking modules.

Results

Expressed CaMKIIβ but Not CaMKIIα Is Enriched in Dendritic Branches and Cell Cortex

We investigated the cellular localization of CaMKIIα versus CaMKIIβ isoforms by constructing CaMKII fusion proteins with GFP (Figure 1A). An earlier study has shown that a GFP–CaMKIIα construct can phosphorylate substrate peptides as well as autophosphorylate itself at threonine 286 (Shen and Meyer, 1998). An additional criterion for functionally intact GFP–CaMKII is the preservation of secondary calcium-independent autophosphorylations at the sites that prevent further calmodulin binding (residues threonine 305 or 306) (Colbran and Soderling, 1990; Hanson and Schulman, 1992). We tested whether the GFP tag on CaMKIIα or CaMKIIβ affects either type of autophosphorylation and determined whether the extent of autophosphorylation is similar to that of the wild-type enzyme. Indeed, wild-type CaMKIIα and GFP-tagged CaMKIIα and CaMKIIβ isoforms showed similar amounts of calcium-dependent and -independent autophosphorylation activity (Figures 1B and 1C).

When GFP-tagged CaMKIIα or CaMKIIβ isoforms were expressed in cultured hippocampal neurons, CaMKIIα was largely homogeneous in the soma and main processes (Figure 1D, left) but was only minimally present in the finer branch structures. In contrast, CaMKIIβ showed a striking enrichment in dendritic branches as well as at the cell cortex (Figure 1D, right). When expressed in rat basophilic leukemia (RBL) cells, CaMKIIα was nearly homogeneously distributed in the cytosol and CaMKIIβ had a distinct cortical localization (Figure 1E, right). The differential distribution of the two isoforms suggests that CaMKIIβ has specific binding interactions in cells that do not occur for CaMKIIα.

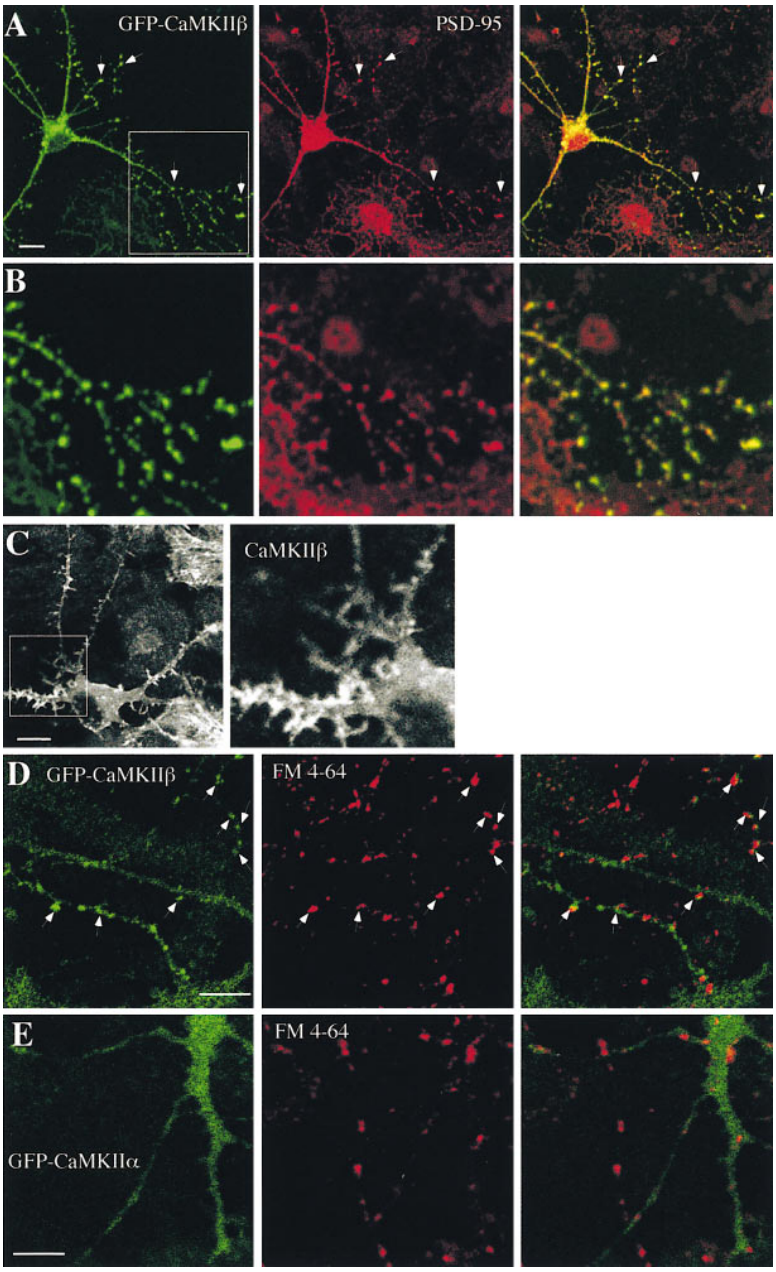

Figure 2. CaMKIIβ Localizes to Dendritic Spines and Filopodia in Neurons

(A) Colocalization of GFP–CaMKIIβ with the PSD marker PSD-95. Cells were fixed and stained with anti–PSD-95 antibodies. The distribution of GFP–CaMKIIβ (green) was then compared to a Cy3-labeled secondary antibody (red) to visualize the distribution of PSD-95. Arrows point to dendritic spines enriched in PSD-95 and GFP–CaMKIIβ.

(B) Magnified region of (A).

(C) In some neurons, a filopodia-like staining by GFP–CaMKIIβ can be observed that is reminiscent of developing dendritic spines (left). At right, a magnified view of such filopodia is shown.

(D) Comparison of the localization of GFP–CaMKIIβ and active presynaptic terminals in living neurons.

(Left) GFP–CaMKIIβ fluorescence (green).

(Center) Subtracted image of presynaptic terminals loaded with FM 4-64 (red).

(Right) Overlay of GFP–CaMKIIβ (green) and active presynaptic terminals (red). Arrows point to locations where the presynaptic marker FM 4-64 is juxtaposed to the localized regions of GFP–CaMKIIβ.

(E) Control measurement, showing the respective distributions of GFP–CaMKIIα (green) and active presynaptic terminals (red) as well as their overlay.

We tested more directly whether CaMKIIβ has more binding interactions than CaMKIIα by comparing the local fluorescence recovery after photobleaching of GFP–CaMKIIβ to that of GFP–CaMKIIα. A 2 μm diameter laser photobleach spot was generated in the cell by a short laser pulse and the fluorescence recovery was monitored by rapid confocal imaging. Consistent with the hypothesis that CaMKIIβ but not CaMKIIα undergoes binding interactions, the recovery after photobleaching was significantly more rapid for CaMKIIα compared to that for CaMKIIβ. This could be quantitatively shown by a calculated average diffusion coefficient of CaMKIIβ that was five times lower than that of CaMKIIα (Figure 1F; see Experimental Procedures for a description of the analysis). Nevertheless, the binding interactions of CaMKIIβ were reversible, since most of the GFP–CaMKIIβ fluorescence recovered on the time scale of 15 s after the laser bleach pulse. Together, these measurements suggest that CaMKIIα expressed alone is a highly mobile protein that has only limited cytosolic binding interactions, while CaMKIIβ is bound in a reversible manner to dendritic and cortical structures.

CaMKIIβ Is an F-Actin–Docking Module Enriched in Dendritic Spines

What are the structures in the dendritic branches and cell cortex targeted by CaMKIIβ? The markedly punctate staining suggested that CaMKIIβ is enriched in dendritic spines. Indeed, an antibody against the postsynaptic protein PSD-95 showed a clear colocalization between GFP–CaMKIIβ (Figure 2A, green) and PSD-95 (red). The arrows in the right panel point to presumed dendritic

spines, which were highly enriched in PSD-95 and GFP–CaMKIIβ (expressed by the yellow color in the overlay image). A magnification of the dendritic region is shown in Figure 2B. Some of the neurons also showed an enriched staining of GFP–CaMKIIβ in filopodia-like branches (Figure 2C) that were reminiscent of developing dendritic spines (Ziv and Smith, 1996). A magnified image of an arbor of such filopodia is shown in the right panel.

We verified that the dendritic spines marked by anti–PSD-95 antibodies and GFP–CaMKIIβ corresponded to mature postsynaptic terminals by comparing the distribution of GFP–CaMKIIβ to that of functional presynaptic terminals. The terminals were marked with the fluorescent synaptic vesicle marker FM 4-64 using a double depolarization protocol (Ziv and Smith, 1996; see Experimental Procedures). Since this type of colocalization study can be performed in living neurons, potential distribution artifacts that may arise during the fixation of neurons can be excluded. When comparing the distribution of GFP–CaMKIIβ (Figure 2D, green) to the location of active presynaptic terminals (represented in red as a difference image of the released FM 4-64 after depolarization), the overlayed image showed a marked juxtaposed localization of GFP–CaMKIIβ and loaded FM 4-64 (Figure 2D, right). This suggests that CaMKIIβ is indeed enriched in mature dendritic spines. In contrast, the uniformly distributed GFP–CaMKIIα was not enriched near active synapses (Figure 2E).

Since actin is highly enriched in dendritic spines and cell cortex (Caceres el al., 1983; Landis and Reese, 1983; Fisher et al., 1998), it is conceivable that the localization of CaMKIIβ to dendritic spines is mediated by a direct or indirect binding interaction of CaMKIIβ with F-actin. We tested the possible colocalization of CaMKIIβ and F-actin in two model cell lines by using rhodamine phalloidin as a marker for polymerized actin (F-actin). In RBL cells, which have predominant cortical F-actin structures, the cortical rhodamine phalloidin closely colocalized with GFP–CaMKIIβ (Figure 3A, GFP–CaMKIIβ in green and rhodamine phalloidin in red). The same nearly complete overlap was also observed in NIH-3T3 cells, which are rich in actin stress fibers (Figure 3B). Again, GFP–CaMKIIβ is shown in green (left) and phalloidin in red (middle), and the overlay image is shown in the right panel. This suggests that the actin cytoskeleton colocalization of CaMKIIβ is not cell type specific.

Further support for the colocalization of CaMKIIβ with F-actin in living cells was obtained by comparing cells before and after treatment with the actin depolarizing drug latrunculin (Spector et al., 1989) (Figure 3C). In RBL cells (top) and fibroblasts (bottom), addition of latrunculin led to a nearly complete loss in the cortical as well as stress fiber staining of GFP–CaMKIIβ.

We then determined biochemically whether expressed CaMKIIβ can bind directly to purified F-actin. Indeed, Met-^{35}S-labeled CaMKIIβ could be effectively sedimented by polymerized actin (Figures 3D, left). In contrast, CaMKIIα is much less sedimentable by polymerized actin using the same assay. Figure 3D, right, shows the counts in each of the bands using a bar diagram (average of five measurements). This suggests that the colocalization of CaMKIIβ with the actin cytoskeleton observed in living cells is the result of a direct and reversible binding interaction between CaMKIIβ and F-actin.

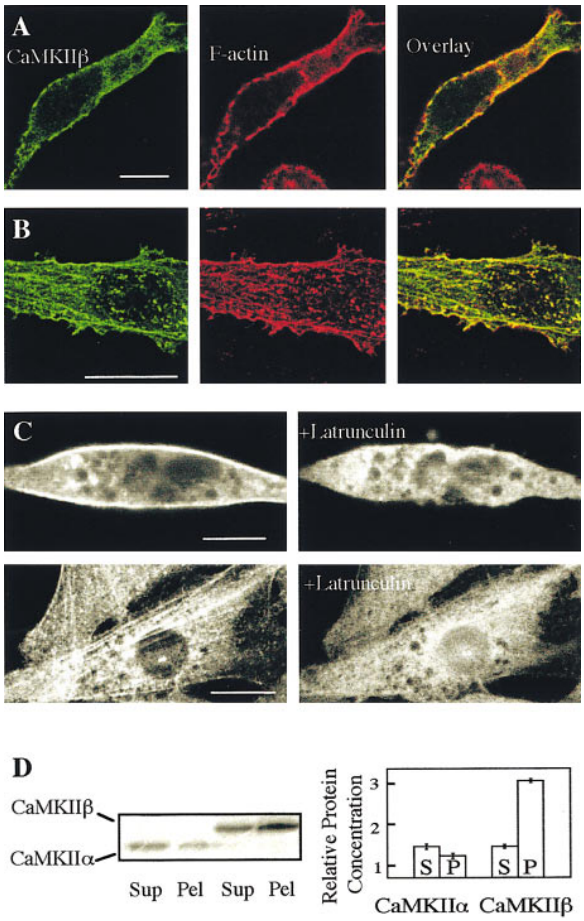

Figure 3. CaMKIIβ Colocalizes with the Cortical Actin Cytoskeleton and Actin Stress Fibers by Binding to F-Actin

(A) Colocalization of GFP–CaMKIIβ (left, green) with rhodamine phalloidin (center, red) in fixed RBL cells. The significant fraction of yellow structures observed in the overlay image (right) is suggestive of a nearly complete colocalization of CaMKIIβ with polymerized actin.

(B) Colocalization of GFP–CaMKIIβ (left, green) with rhodamine phalloidin (center, red) in fixed NIH-3T3 cells. Again, a nearly complete colocalization is apparent from the yellow color of stress fibers (right).

(C) The cortical distribution of GFP–CaMKIIβ in RBL cells is disrupted by latrunculin (top) (50 μM, 2 min). The stress fiber staining is disrupted by latrunculin (bottom) (50 μM, 2 min). Calibration bars, 5 μm.

(D) CaMKIIβ directly binds to purified F-actin. Nonmuscle G-actin was polymerized at concentration of 150 μg/ml (left). In vitro translated CaMKII isoforms were added and incubated on ice for 1 hr followed by centrifugation at 100,000 × g for 30 min. The pellet and supernatant were resolved by SDS-PAGE and exposed on a Phosphorimager. CaMKIIβ is significantly enriched in the actin pellet when compared to CaMKIIα (right) (average of five experiments).

CaMKIIα Is Targeted to Dendritic Spines When Coexpressed with CaMKIIβ

We then tested whether the coexpression of CaMKIIα and CaMKIIβ in the same cell affects their respective localization. An effective coexpression of both isoforms was made possible by using an RNA transfection method. In this approach, a large number of translation-competent RNA molecules are directly introduced into

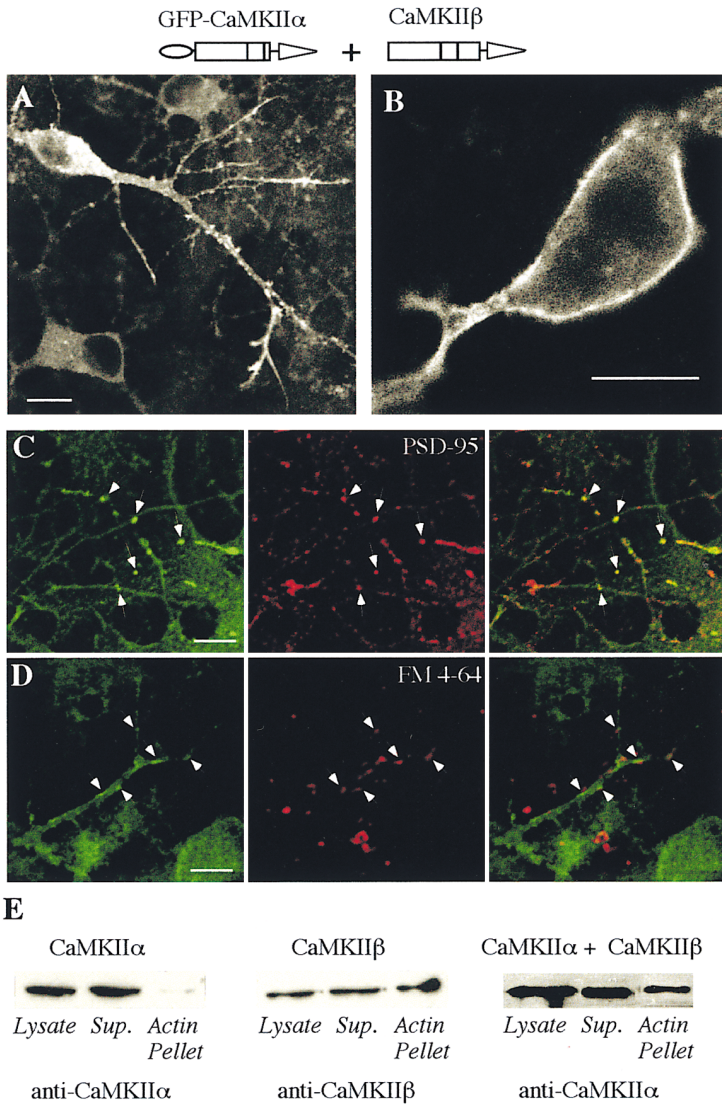

Figure 4. CaMKIIα Is Targeted to the Actin Cytoskeleton When Expressed in the Same Cell with CaMKIIβ

(A) Coexpression of GFP–CaMKIIα together with CaMKIIβ without a GFP tag in a CA1–CA3 neuron.

(B) Coexpression of GFP–CaMKIIα together with CaMKIIβ without a GFP tag in RBL cells.

(C) Comparison of the localization of GFP–CaMKIIα, expressed together with CaMKIIβ, to the PSD marker PSD-95. Cells were fixed and stained with anti–PSD-95 antibodies. The distribution of GFP–CaMKIIα (green) was compared to a Cy3-labeled secondary antibody (red) to visualize the distribution of PSD-95. Arrows point to dendritic spines enriched in PSD-95 and GFP–CaMKIIα.

(D) Localization of GFP–CaMKIIα (mixed with CaMKIIβ RNA) compared with active presynaptic terminals in living neurons.
(Left) GFP–CaMKIIα fluorescence (green).
(Center) Subtracted FM 4-64 staining as described in Figure 2.
(Right) Overlay of the two images. Arrows highlight regions where GFP–CaMKIIα (mixed with CaMKIIβ RNA) and active presynaptic terminals are juxtaposed to each other. Calibration bars, 10 μm.

(E) Western blots of supernatant and actin pellet fractions of NIH-3T3 cells expressing CaMKIIα, CaMKIIβ, or CaMKIIα + CaMKIIβ, respectively.
(Left) An anti-CaMKIIα antibody identified most of the expressed CaMKIIα in the supernatant and only a minimal amount in the actin-enriched pellet (see Experimental Procedures section).
(Center) An anti-CaMKIIβ antibody identified a significant fraction of expressed CaMKIIβ in the actin pellet.
(Right) In cells coexpressing CaMKIIα and CaMKIIβ, an anti-CaMKIIα antibody identified a significant fraction of CaMKIIα in the actin pellet, supporting the hypothesis that CaMKIIβ targets CaMKIIα to F-actin.

the cytosol of adherent cells by microporation (Yokoe and Meyer, 1996; Teruel and Meyer, 1997). Thus, RNA encoding different proteins can be mixed and expressed at a defined ratio within each transfected cell. Strikingly, when GFP–CaMKIIα was expressed together with CaMKIIβ (without a GFP tag) in hippocampal neurons, GFP–CaMKIIα became associated with the same dendritic spine and cortical structures (Figure 4A). A largely cortical localization of GFP–CaMKIIα was also observed in RBL cells in the presence of CaMKIIβ (Figure 4B). In contrast, expression of CaMKIIα (without a GFP tag) together with a similar amount of GFP–CaMKIIβ did not affect the cortical localization of GFP–CaMKIIβ (data not shown). Using the same colocalization protocols as described before in Figure 2, we also found a marked colocalization between GFP–CaMKIIα, coexpressed with CaMKIIβ, and anti PSD-95 antibodies (Figure 4C). In living neurons, GFP–CaMKIIα, coexpressed with CaMKIIβ, showed a marked localization juxtaposed to the presynaptic marker FM 4-64 (Figure 4D).

Can this effect of CaMKIIβ on CaMKIIα localization be confirmed biochemically? We used a detergent extraction procedure of NIH-3T3 cells to test whether CaMKIIβ and/or CaMKIIα could be found in an actin-enriched pellet fraction. This extraction protocol has been shown to significantly enrich for actin and actin binding proteins (Egelhoff et al., 1991). Expressed CaMKIIβ and CaMKIIα isoforms without a GFP tag were used for these measurements. In agreement with the in vivo data, CaMKIIα, when expressed alone, was largely absent from the actin pellet, while CaMKIIβ was highly enriched in the actin pellet (Figure 4E, left and center). When both isoforms were expressed together, a significant fraction of CaMKIIα was found in the actin cytoskeletal fraction (Figure 4E, right). Taken together, these studies are consistent with a targeting mechanism by which CaMKIIα is localized to F-actin if expressed together with a sufficient amount of CaMKIIβ.

How does CaMKIIβ target CaMKIIα to the actin cytoskeleton? A likely hypothesis is that CaMKIIα does not undergo cytoskeletal binding interactions of its own but binds to CaMKIIβ, which then anchors the complex to

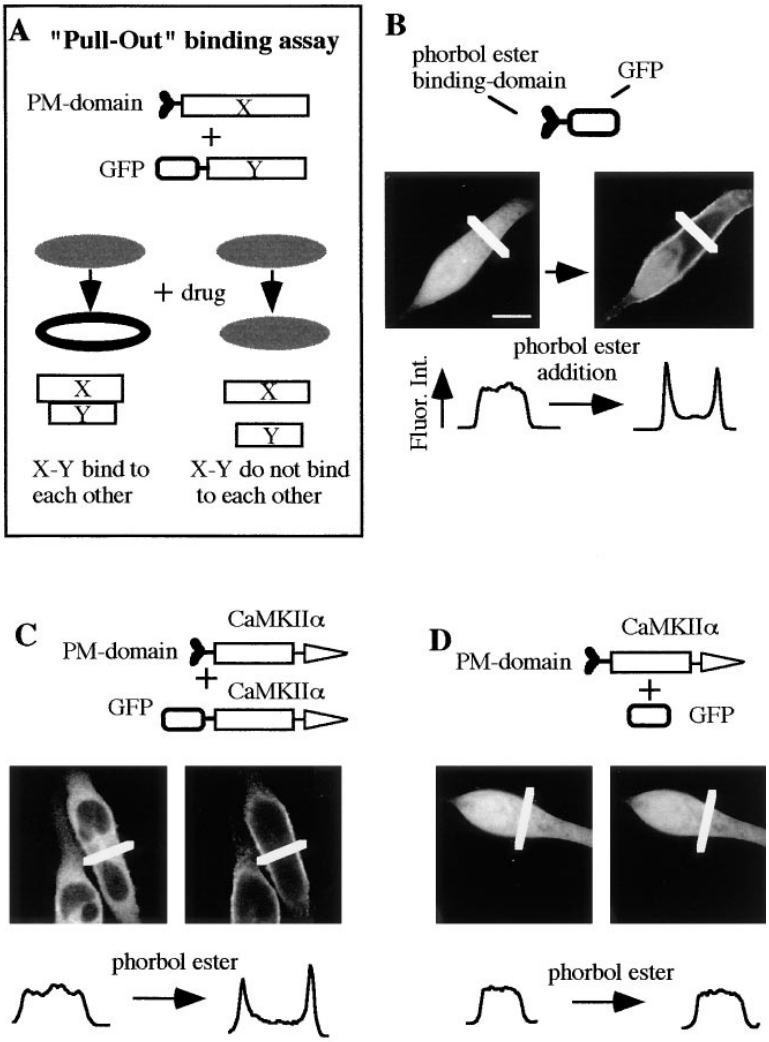

Figure 5. Development of a Pull-Out Binding Assay to Study Protein–Protein Interactions in Living Cells

(A) Principle of the Pull-Out binding assay. The binding interaction between a Protein X and Protein Y can be measured by tagging Protein X with an inducible plasma membrane binding domain (PM domain) and Protein Y with GFP. If a significant fraction of the two proteins bind to each other, drug addition targets the GFP to the plasma membrane. In contrast, the cytosolic distribution remains unaltered if Protein X and Y do not bind to each other.

(B) Property of a minimal phorbol ester binding domain used as an inducible PM domain in the Pull-Out binding assay. A fusion protein between GFP and the phorbol ester binding domain can be pulled from the cytosol to the plasma membrane by addition of phorbol ester.

(Left) Distribution of the fusion protein before phorbol ester addition.

(Right) Distribution of the fusion protein after phorbol ester addition.

(Bottom) Line scans of the fluorescence intensity across the cell before and after phorbol ester addition.

(C) Demonstration that nearly all CaMKIIα molecules are part of oligomers. Phorbol ester addition to cells with coexpressed PM–CaMKIIα and GFP–CaMKIIα leads to the near complete plasma membrane translocation of GFP–CaMKIIα.

(D) Control measurements showing that expressed GFP itself is not affected by phorbol ester addition. Calibration bars, 10 μm.

F-actin. To understand this heterologous CaMKII targeting mechanism, several important questions about the binding interaction and oligomerization of CaMKIIα and CaMKIIβ have to be answered. First, can CaMKIIβ form oligomers on its own and, if it does, how large are these oligomers compared to those formed by CaMKIIα? Second, do coexpressed CaMKIIα and CaMKIIβ isoforms assemble into hetero- or homooligomers in living cells? Third, if they form heterooligomers, does the incorporation of CaMKIIβ into CaMKIIα oligomers occur as a stochastic process? Fourth, what minimal ratio of CaMKIIβ to CaMKIIα is required for targeting CaMKIIα to the actin cytoskeleton?

Oligomer Formation Can Be Explored in Living Cells Using a GFP-Based Pull-Out Binding Assay

To address the question of homo- versus heterooligomer formation, we developed an assay to quantitatively study protein–protein binding interactions in living cells (Pull-Out binding assay; Figure 5A). Our strategy was to use a protein domain (PM domain) that translocates to the plasma membrane in response to the addition of a drug. The potential binding interaction between the investigated Protein X and Protein Y could then be investigated by fusing this PM domain to Protein X and a GFP tag to Protein Y (or vice versa). Both fusion proteins could then be expressed in the same cell and their binding interaction investigated. First, if the initially cytosolic GFP–Protein Y remains cytosolic after drug addition, no significant binding interaction occurs between Proteins X and Y. Second, if the drug addition leads to the GFP–Protein Y translocation to the plasma membrane (along with the nonfluorescent PM–Protein X), Proteins X and Y bind to each other.

We used the first phorbol ester binding domain of protein kinase C as such a PM domain. This small 6 kDa domain is an initially cytosolic protein that binds nearly irreversibly to the plasma membrane after phorbol ester addition (Oancea et al., 1998). The distinct property of this domain is shown in Figure 5B. Before phorbol ester addition, a fusion protein of the phorbol ester binding domain with GFP is a cytosolic protein (left) that is "pulled" from the cytosol to the plasma membrane after addition of phorbol ester (right). This translocation process occurs in less than a minute and is mediated by a diffusion-dependent high affinity binding interaction of

the fusion protein with plasma membrane–localized phorbol ester (Oancea et al., 1998). It should be noted that the also visible nuclear-localized GFP fusion protein translocates to the plasma membrane much more slowly due to its slow diffusion through nuclear pores.

We first used this PM domain to determine whether most of the expressed CaMKIIα isoforms is present in an oligomeric state. To test for oligomerization in vivo, PM-tagged CaMKIIα and GFP–CaMKIIα were expressed in the same cell (Figure 5C, left). As expected, addition of phorbol ester led to a marked translocation of the initially cytosolic GFP–CaMKIIα to the plasma membrane (Figure 5C, right). This change in the distribution before and after addition of phorbol ester can be more quantitatively measured in a line profile analysis comparing the fluorescence intensity across the cell before and after phorbol ester addition (Figure 5C, bottom). In control experiments, GFP alone was coexpressed with PM-tagged CaMKIIα, and no plasma membrane translocation of GFP was observed after phorbol ester addition (Figure 5D). The finding that most GFP–CaMKIIα is pulled to the plasma membrane by PM–CaMKIIα strongly suggests that most of the expressed CaMKIIα is present in the cell in an oligomeric state.

CaMKIIβ Homooligomers Are Significantly Smaller Than CaMKIIα Homooligomers

While CaMKIIα has been proposed to be an homooligomer with 8–12 subunits, it is controversial if CaMKIIβ forms oligomers and how large these potential oligomers are (Yamauchi et al., 1989). To measure the apparent oligomer sizes of CaMKIIα and CaMKIIβ in living cells, we expressed GFP–CaMKII together with a decreasing amount of PM–CaMKII and measured the phorbol ester–induced translocation to the plasma membrane (a schematic view of the expected oligomer translocation process is shown in Figure 6A). Since the phorbol ester-induced plasma membrane affinity of the PM domain is nearly irreversible, it is likely that a single subunit of PM–CaMKIIα is sufficient to induce the plasma membrane translocation of a CaMKIIα oligomer. As discussed above, the RNA transfection method allows one to quantitatively titrate the amount of the two CaMKII fusion proteins in the same cell. To determine the respective expression levels for the two microporated RNA species, the concentration of the translated proteins was measured in parallel by in vitro translation of the same RNAs in the presence of [^{35}S]Met (Figure 6B).

Figure 6C shows the GFP–CaMKIIα plasma membrane translocation at increasing dilutions of coexpressed PM–CaMKIIα. The left images show the distribution before and the right images after phorbol ester addition. Interestingly, the phorbol ester–induced targeting to the plasma membrane was still measurable when PM–CaMKIIα was diluted to $<$3% of GFP–CaMKIIα. The sequential reduction in plasma membrane translocation can be seen more clearly in fluorescence line intensity traces (Figure 6D). The loss in phorbol ester–mediated plasma membrane targeting at increasing PM–CaMKIIα dilutions was analyzed by dividing the relative plasma membrane fluorescence intensity of GFP–CaMKIIα (Δ_{PM}) by the average cytosolic fluorescence intensity before phorbol ester addition (I_{pre}) (Figure 6E). A Δ_{PM}:I_{pre} ratio of 0 indicates that no plasma membrane translocation occurred, and a PM:I_{pre} ratio of $\sim$3 corresponds to the translocation observed for the PM–GFP construct itself.

Based on this analysis, a titration curve can be obtained, showing the relative plasma membrane translocation at decreasing dilution ratios of PM–CaMKIIα to GFP–CaMKIIα (Figure 6F). A 50% reduction in plasma membrane targeting was observed at an approximate dilution ratio of 1 PM–CaMKIIα per 14 GFP–CaMKIIα. A Poisson distribution model would predict that the probability (p) to introduce at least one subunit into an oligomer with N subunits is $p = 1 - (R/[R + 1])^N$, with R as the dilution ratio. Using this model, a best fit to the data was obtained for $N = 13.5$, in close agreement with a previous estimate of 12 subunits for purified CaMKIIα (Yamauchi et al., 1989; Kanaseki et al., 1991).

We then used the same approach to determine if CaMKIIβ forms oligomers. Although GFP–CaMKIIβ has a partial cortical and internal F-actin localization, this binding interaction was reversible, and a much more pronounced plasma membrane localization can be induced by addition of phorbol ester to a PM-tagged CaMKIIβ. Using this phorbol ester–triggered increase in plasma membrane translocation of GFP–CaMKIIβ, a titration curve was obtained for the relative plasma membrane translocation at decreasing dilution ratios of PM–CaMKIIβ to GFP–CaMKIIβ. Interestingly, the apparent average size of CaMKIIβ oligomers was 4.2, significantly smaller than that of the α isoform (Figure 6F). Thus, these in vivo measurements clearly show that CaMKIIβ can form oligomers, albeit with a significantly smaller apparent size than those formed by CaMKIIα. This apparent size of CaMKIIβ oligomers was consistent with our finding that CaMKIIβ purified from baculovirus–transfected Sf9 cells had a size much smaller than that of CaMKIIα expressed by the same method (K. S., unpublished data).

CaMKIIα and CaMKIIβ Form Stochastic Heterooligomers

Since the relative expression of CaMKIIα to CaMKIIβ is highly variable between different types of neurons, we determined how efficient heterooligomer formation is compared with homooligomer formation. We pursued the same dilution approach as described in Figure 6 but for the heterooligomers. The calculated line plots in Figure 7A show the curves expected for the insertion of PM–CaMKIIβ into GFP–CaMKIIα oligomers for a stochastic insertion mechanism (dashed curve). The measured relative plasma membrane translocation for decreasing ratios of PM–CaMKIIβ to GFP–CaMKIIα closely matched a predicted stochastic insertion mechanism. The same measurements were then made for PM–CaMKIIα insertion into GFP–CaMKIIβ oligomers by dilution of the PM–CaMKIIα fusion protein at a constant concentration of CaMKIIβ (Figure 7B). The calculated curve for a stochastic insertion mechanism is overlapping with the fitted one.

Together, this titration approach suggests that if CaMKIIα and CaMKIIβ isoforms are expressed at the

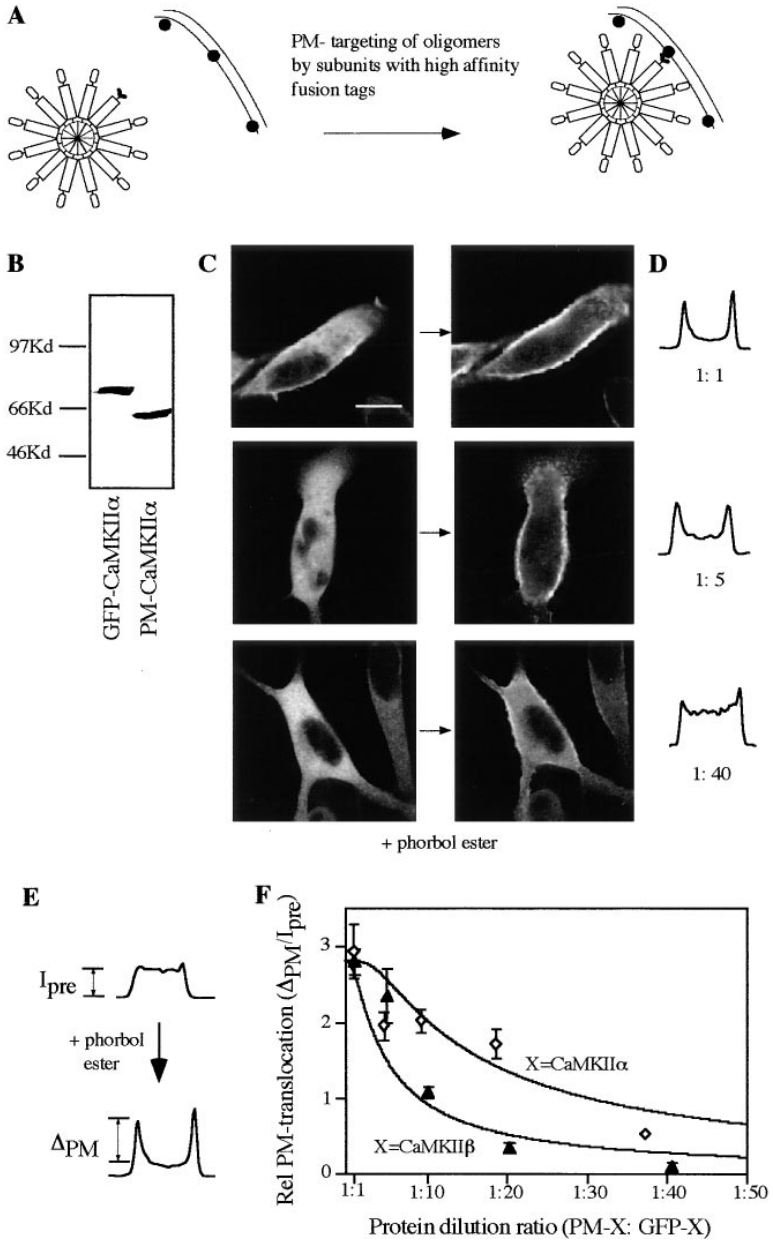

Figure 6. CaMKIIα Forms Larger Oligomers Than CaMKIIβ

(A) Schematic representation of the assay to measure the size of CaMKIIα and CaMKIIβ oligomers in living cells.

(B) Quantitative comparison of the concentrations of expressed GFP–CaMKIIα and PM–CaMKIIα measured by in vitro translation. The relative concentration of the expressed proteins was compared by [^{35}S]Met incorporation into in vitro translated proteins. The same RNA was used for the in vitro translation and the RNA transfection of cells.

(C) Only for dilutions below 10% does PM–CaMKIIα begin to lose its potency to translocate GFP–CaMKIIα to the plasma membrane. Dilutions were achieved by mixing the RNAs for PM–CaMKIIα and GFP–CaMKIIα at decreasing ratios.

(Top and center) Plasma membrane translocation is still near maximal at dilutions of 1:1 and 1:5.

(Bottom) Plasma membrane translocation is markedly reduced at a 1:40 dilution. Calibration bars, 10 μm.

(D) Line scan profiles of three different dilutions after phorbol ester addition.

(E) Schematic representations of the quantitative analysis used to measure the relative plasma membrane translocation. I_{pre} and PM are measured before and after PMA addition, respectively.

(F) Plot of the relative plasma membrane translocation of CaMKIIα and CaMKIIβ at decreasing ratios of expressed PM–CaMKII and GFP–CaMKII. Each point is an average of at least 10 experiments. The solid curves are best fits to the two set of data, and the dashed lines show the confidence interval. Best fits were obtained assuming an average of 13.5 subunits for CaMKIIα and 4.2 subunits for CaMKIIβ.

same time and place, they form mixed oligomers with a stochastic probability for the insertion of either one of the isoforms. This also suggests that most CaMKII oligomers in neurons contain a variable fraction of CaMKIIβ that is defined by the relative expression level of locally translated CaMKIIβ versus CaMKIIα. For the physiological situation, it is then important to know how many CaMKIIβ isoforms have to be inserted into mostly CaMKIIα heterooligomers to still effectively target CaMKII to its cytoskeletal docking site.

A Small Number of CaMKIIβ Isoforms Are Sufficient to Target CaMKII Heterooligomers to the Actin Cytoskeleton

While the previous studies were useful to dissect the oligomer formation of CaMKIIα and CaMKIIβ, they did not resolve whether individual or multiple CaMKIIβ subunits are required for the targeting of CaMKIIα/β heterooligomers to the actin cytoskeleton. We used the same RNA dilution strategy to determine at which ratio of GFP–CaMKIIα to CaMKIIβ the cytoskeletal localization still occurs. The distinct cortical actin cytoskeleton localization of CaMKIIβ in RBL cells was used in this assay (Figure 7C). While CaMKIIβ was less potent in targeting GFP–CaMKIIα to the plasma membrane than the PM–CaMKII constructs, 50% translocation to the cortical actin cytoskeleton required a ratio of ~6.5:1 of GFP–CaMKIIα to CaMKIIβ. Since CaMKIIα isoforms contain ~13 subunits, this suggests that a small number of CaMKIIβ subunits are sufficient to target CaMKIIα/β heterooligomers to the actin cytoskeleton.

In a second independent approach to understand the

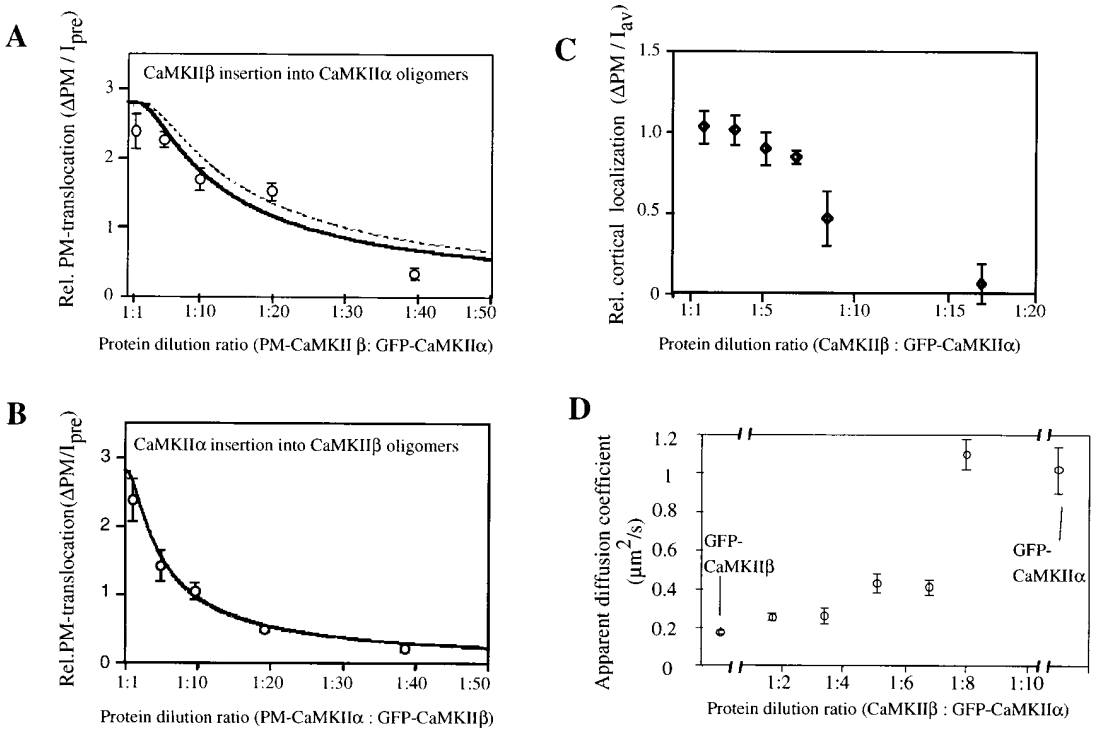

Figure 7. Requirement for More Than One CaMKIIβ Subunit for Targeting CaMKIIα/β Heterooligomers to the Actin Cytoskeleton

(A) Insertion of CaMKIIβ into heterooligomers of mostly CaMKIIα is a stochastic process. The panel shows a plot of the relative plasma membrane translocation of GFP–CaMKIIα at decreasing ratios of expressed PM–CaMKIIβ. Each point is an average of at least ten experiments. The dashed line shows the predicted curve for a stochastic insertion of PM–CaMKIIβ into heterooligomers ($p = 1 - [R/(R + 1)]^N$ with R as the dilution ratio and N as the number of subunits; since the PM domain induces a nearly irreversible membrane binding interaction, it was assumed that one PM domain per oligomer is sufficient for inducing translocation).

(B) The insertion of CaMKIIα into heterooligomers with mostly CaMKIIβ is a stochastic process. The panel shows a plot of the relative plasma membrane translocation of GFP–CaMKIIα at decreasing ratios of expressed PM–CaMKIIβ. Each point is an average of at least ten experiments. The predicted curve for a stochastic insertion of PM–CaMKIIα into CaMKIIβ oligomers overlaps with the fit of the data.

(C) Relative cortical localization of GFP–CaMKIIα plotted as a function of increasing dilutions of CaMKIIβ. Relative cortical localization is defined as Δ_{PM}/I_{av}, with Δ_{PM} as the intensity difference between the PM and the cytosol and I_{av} as the average fluorescence intensity of a particular cell. Each point is an average of at least ten experiments.

(D) Measurement of the change in the diffusion coefficient as a function of an increasing dilution of CaMKIIβ to GFP–CaMKIIα. The apparent diffusion coefficient of GFP–CaMKIIα increased from 0.2 to 1 $\mu m^2/s$ as the ratio of CaMKIIβ to CaMKIIα was lowered from 1:2 to 1:9. The outermost left and right data points show the diffusion coefficients of GFP–CaMKIIβ and GFP–CaMKIIα, respectively.

cytoskeletal targeting of CaMKIIα by CaMKIIβ, we measured the binding interactions of the heterooligomers by measuring their diffusion coefficients. As shown in Figure 1F, GFP–CaMKIIα has a 5-fold faster apparent diffusion than GFP–CaMKIIβ. Diffusion coefficients were then measured at increasing dilutions of GFP–CaMKIIα to CaMKIIβ. Similar to the results with the localization to the cortical cytoskeleton, the diffusion coefficient of CaMKIIα was reduced by 50% when the concentration of CaMKIIβ exceeded 15% of that of GFP–CaMKIIα (Figure 7D). Together, these measurements show that CaMKIIβ is a potent targeting domain that can localize a much larger number of CaMKIIα isoforms to the actin cytoskeleton.

Discussion

Functional Importance of Docking CaMKII to F-Actin in Dendritic Spines and Cell Cortex

What is the functional advantage of a subcellular localization of CaMKII? The main advantages of localizing enzymes and signaling proteins are (1) increased efficiency and (2) increased specificity. By targeting CaMKII to dendritic spines, its local concentration is elevated and the efficiency of substrate phosphorylation is increased. Important dendritic substrates of CaMKII include AMPA receptors, NMDA receptors, SynGAP, and MAP2.

Hence, by localizing CaMKII to dendritic spines, the kinase can more effectively exert its functions in synaptic plasticity. The postsynaptically localized AMPA receptor has been shown to be an important substrate of CaMKII, and phosphorylation by CaMKII increases the AMPA receptor conductivity 3-fold (McGlade-McCulloh et al., 1993; Barria et al., 1997). This upregulation of the AMPA receptor is thought to be one of the critical functions of CaMKII in synaptic plasticity (Nicoll and Malenka, 1995). The postsynaptically localized NMDA receptor has also been shown to be a substrate for CaMKII (Omkumar et al., 1996), although the function of the NMDA receptor phosphorylation by CaMKII is not well understood. Furthermore, the NMDA receptor has

been shown to bind to α-actinin, an actin binding protein present in PSDs (Wyszynski et al., 1997). A recent study also suggested that CaMKII has an important postsynaptic role in inhibiting the activity of the PSD protein SynGAP, a Ras-GTPase activating protein that is likely important in regulating the dendritic MAP kinase pathway (Chen et al., 1998).

The dendritic tubulin binding protein MAP2 is a major CaMKII substrate and is known to form a bridge between actin and tubulin. Phosphorylation by CaMKII has been shown to break its binding interaction with actin, which is potentially important for a reorganization of the dendritic morphology (Vallano et al., 1986). An important role of CaMKII in stabilizing dendritic branches has been suggested in recent studies of neurons using expressed catalytically active CaMKII (Wu and Cline, 1998).

In addition to its postsynaptic functions, CaMKII may also be relevant for regulation of the presynaptic actin binding protein synapsin 1. It is likely that the direct association of CaMKII with F-actin is important for the enhancement of synapsin 1 phosphorylation by CaMKII. Functionally, phosphorylation by CaMKII has been shown to disable the synapsin–actin binding interaction and thereby enables synaptic vesicles to become available for secretion (Llinas et al., 1991; Benfenati et al., 1992).

Finally, biochemical evidence suggests that a significant fraction of CaMKII is enriched in postsynaptic densities (PSDs). This structure has been shown to contain a marked amount of CaMKIIα and a lesser amount of actin and CaMKIIβ in hippocampal neurons. Interestingly, CaMKIIβ and actin are present in PSDs at about the same molar concentration (Kelly and Vernon, 1985), making it possible that CaMKII localization to dendritic spines is mediated by a direct CaMKIIβ–actin interaction. Furthermore, studies by McNeill and Colbran (1995) and Strack et al. (1997) have shown that CaMKII, once autophosphorylated, can bind to at least two postsynaptic density proteins of 140 and 190 kDa. In light of the data in our study, it is conceivable that CaMKII oligomers are initially prelocalized to the PSD by their reversible actin binding interaction but then switch their PSD binding partner or further translocate to PSDs following CaMKII autophosphorylation.

Role of CaMKIIβ As an F-Actin Targeting Module

Our study shows that CaMKIIβ functions as a targeting module that localizes CaMKIIα/β heterooligomers to dendritic spines and other F-actin rich regions. Where is the structural sequence motif for heterooligomerization? Earlier studies suggested that the motif for oligomerization of CaMKII is located at its C terminus (Yamauchi et al., 1989). This domain is 78% identical between CaMKIIα and CaMKIIβ. At least for CaMKIIα, a C-terminal, 135 amino acid sequence of CaMKIIα was shown to be necessary and sufficient for oligomer formation (Shen and Meyer, 1998). Deletions of more than 8 amino acids at the C terminus and more than 21 amino acids at the N-terminal end of this short domain were sufficient to abolish oligomerization. Using the Pull-Out binding assay as an in vivo approach, we now confirmed that minimal C-terminal domains of CaMKIIα and CaMKIIβ are indeed sufficient for oligomer formation. In these measurements, constructs encoding GFP- and PM-tagged minimal oligomerization domains of CaMKIIα and CaMKIIβ were coexpressed at different ratios (K. S., unpublished data).

The heterologous targeting mechanism is particularly interesting since only 15% of CaMKIIβ was needed to bind 50% of CaMKII heterooligomers to the actin cytoskeleton. Thus, cells can potentially control the localization of the predominant CaMKIIα isoforms by regulating the local expression of CaMKIIβ. The different relative expression levels of CaMKIIβ during development and in different neuronal cell types suggests that this targeting mechanism is physiologically important and may be responsible for a distinct subcellular localization of CaMKII in different cell types and periods of development. A cell type–specific difference in CaMKII attachment is consistent with the earlier finding that a much smaller fraction of CaMKII is found in the soluble fraction of isolated cerebellum than in the soluble fraction of the forebrain (10% versus 50%) (Kelly and Vernon, 1985; Kelly et al., 1987). This is paralleled by a ratio of CaMKIIβ to CaMKIIα of 4:1 and 1:3, respectively, in these two brain regions (Miller and Kennedy, 1985).

An intriguing piece in the puzzle is the observation that CaMKIIα can be locally translated in dendrites (Burgin et al., 1990). It suggests that a spatially distinct expression of CaMKIIα and CaMKIIβ within a cell could be used to regulate the isoform ratio of the assembled heterooligomer and thereby control the fraction of CaMKII activity associated with F-actin.

Since a variable fraction of expressed CaMKIIβ is present as a spliced variant CaMKIIβ′, we also tested the localization of GFP-tagged CaMKIIβ′. Interestingly, CaMKIIβ′ showed a markedly lower F-actin localization than CaMKIIβ (K. S., unpublished data). Thus, the F-actin localization of CaMKIIα/β heterooligomers can be regulated not only by the respective expression of CaMKIIα and CaMKIIβ but also by the alternative splicing of CaMKIIβ.

Together, these results suggest that if CaMKIIα and CaMKIIβ are translated at the same time and in the same location, they form random heterooligomers that are docked to F-actin. When taking into account the lower F-actin affinity of the alternatively spliced variant of CaMKIIβ, a critical number for docking CaMKII activity to the actin cytoskeleton is the local expression of CaMKIIβ versus the sum of CaMKIIα plus CaMKIIβ′.

Heterologous Targeting Model for CaMKII

Could the cytoskeletal targeting of CaMKIIα by CaMKIIβ be an example for a more general heterologous targeting mechanism (Figure 8)? This question is particularly intriguing since the family of CaMKII isoforms has recently been expanded with the cloning of CaMKIIγ and CaMKIIδ as well as the identification of a large number of splice variants including CaMKIIβ′, CaMKIIα_B, CaMKIIδ_A, and CaMKIIδ_B (Braun and Schulman, 1995). If a heterologous targeting mechanism would exist for all isoforms, CaMKIIα should also form heterooligomers with CaMKIIγ and CaMKIIδ isoforms. Indeed, when we expressed PM–CaMKIIα together with GFP-tagged CaMKIIγ and CaMKIIδ isoforms, a direct binding interaction could be demonstrated using the Pull-Out binding assay (K. S., unpublished data). Thus, the coexpression of CaMKIIα,

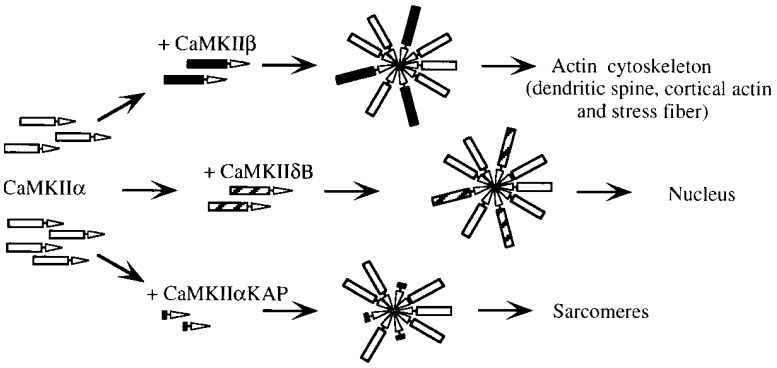

Figure 8. Heterologous Targeting Model for CaMKII

The model predicts that the localization of the predominant CaMKII isoform (CaMKIIα in many neurons) is regulated by the relative expression level of CaMKIIβ and possibly other targeting CaMKII isoforms and splice variants such as CaMKIIβ′, CaMKIIδ_B and CaMKIIαKAP. The latter two isoforms may target CaMKIIα or other nonlocalized CaMKII isoforms to the nucleus or sarcomere structures in different cell types. CaMKIIα and other nonlocalized CaMKII isoforms would then serve as "amplifiers" that enhance the local activity of CaMKII in cell-specific regions defined by the expression of the actual targeting isoforms. Thus, the specificity and efficiency of substrate phosphorylation by CaMKII heterooligomers could be controlled by the local cotranslation of dedicated targeting isoforms.

CaMKIIβ, CaMKIIγ, and CaMKIIδ can likely generate functional heterooligomers that contain all possible combinations of CaMKII isoforms.

While all of these CaMKII isoforms have a conserved oligomerization domain, they contain a variable region that is inserted between the oligomerization domain and the regulatory domain. At least for the CaMKIIα_B and CaMKIIδ_B isoforms, this insert includes a nuclear localization sequence that targets these two CaMKII variants to the nucleus (Srinivasan et al., 1994; Brocke et al., 1995). Thus far, one example is known where the catalytic and regulatory domain has been deleted and only a core oligomerization domain (CaMKIIα) and a variable region are left in the catalytically incompetent protein (Bayer et al., 1996; Sugai et al., 1996). This cardiac α KAP protein (CaMKIIαKAP) is localized to the sarcomere structures and is likely to serve as a "pure" targeting module that lacks a catalytic domain of its own. Using the different subcellular localization to the actin cytoskeleton, nucleus, and sarcomeres as examples, we propose that many of the isoforms and splice variants have a specific role in localizing CaMKII heterooligomers to particular cellular sites. In this model, the selectivity and efficiency of CaMKII action can be controlled by increasing or decreasing the expression of a less abundant "targeting isoform" such as CaMKIIβ. Taken together, the formation of large heterooligomers between CaMKII isoforms and the presence of different CaMKII "targeting isoforms" strongly suggests that localization of CaMKII through "heterologous targeting" is a general mechanism to control the efficiency and specificity of CaMKII function.

Experimental Procedures

Cloning of CaMKII Fusion Constructs

The cDNA for rat CaMKIIα, CaMKIIβ, and CaMKIIβ′ were generous gifts from Dr. Howard Schulman. The construction of the GFP–CaMKIIα vector was described previously (Shen and Meyer, 1998). To obtain the in vitro transcription vector for CaMKIIα without GFP, the CaMKIIα cDNA was amplified by PCR and cloned into the in vitro transcription vector δSHiro3. DNA sequencing were performed to exclude PCR errors. GFP–CaMKIIβ and CaMKIIβ were also cloned into the SHiro3 and δSHiro3 vectors using a similar PCR strategy. The construction of PM–GFP or Cys–GFP was described previously (Oancea et al., 1998). PM–CaMKIIα and PM–CaMKIIβ were made by replacing the GFP sequence with CaMKIIα and CaMKIIβ coding sequence in the same SHiro3 vector.

In Vitro Translation

In vitro translation with SP6 RNA polymerase was performed according to the manufacturer's protocol using a commercial kit (TNT-coupled reticulocyte lysate system, Promega). In vitro transcription reactions were performed using mRNAs as templates. The relative molar concentration of the different translated proteins was calculated by calibration using [^{35}S]Met incorporation and by counting the number of methionines in the respective protein. Nonradioactive Met was used to obtain CaMKIIs and fusion constructs for the autophosphorylation assay.

Ca^{2+}-Dependent and -Independent Autophosphorylation of CaMKII and GFP Fusion Proteins

CaMKII autophosphorylation assays were performed as described previously (Hanson et al., 1994). Briefly, CaMKII isoforms and fusion constructs were autophosphorylated at 30°C in 25 μl reactions containing 50 mM PIPES (pH 7.0), 10 mM $MgCl_2$, 500 μM $CaCl_2$, 600 nM calmodulin, 50 μg/ml BSA, and 200 μM [γ-^{32}P]ATP (6000 cpm/pmol). The Ca^{2+}-dependent autophosphorylation reaction was started by adding in vitro translation product into the reaction mix and stopped by addition of EDTA (16.7 mM final concentration) 30 s later. To measure the extent of the Ca^{2+}-independent autophosphorylation, a 30 s reaction at high Ca^{2+} was followed by a 120 s secondary incubation in the presence of added EGTA (3.3 mM final concentration). In control experiments, 3.3 mM EGTA were included in the initial reaction mix. The reaction mix was then resolved by SDS-PAGE and subjected to Phosphorimager analysis. The densitometry of bands were measured and corrected by the amount of kinase, which was determined in a separate in vitro translation reaction with [^{35}S]Met as described above.

In Vitro Transcription and RNA Processing

In vitro transcription and RNA processing were performed as described previously (Yokoe and Meyer, 1996; Shen and Meyer, 1998). Briefly, in vitro transcription with SP6 RNA polymerase was performed according to the manufacturer's protocol using a commercial kit (mMESSAGE mMACHINE, Ambion). 10 mM EDTA was used to terminate the reaction. RNA was purified by column chromatography (RNeasy column, Qiagen) followed by the addition of a poly(A) tail. Poly adenylation was carried out for 30 min at 37°C in a 50 μl reaction mixture containing 40 mM Tris-HCl (pH 8.0), 10 mM $MgCl_2$, 2.5 mM $MnCl_2$, 250 mM NaCl, 0.25 mg/μl RNA, 250 mM ATP, and 5 U poly(A) polymerase (Life Technologies). The reaction was terminated by addition of 20 mM EDTA. Unincorporated ATP and salts were removed by applying the mRNA to a RNeasy column. The eluent was dried and mRNA was dissolved at 1 μg/μl in the electroporation buffer (5 mM KCl, 125 mM NaCl, 20 mM HEPES [pH 7.4], and 10 mM glucose).

Cell Culturing and Electroporation

RBL 2H3 cells were maintained in Dulbecco's Minimum Essential Medium (DMEM) supplemented with 20% fetal bovine serum (Life Technologies, Gaithersburg, MD) at 37°C with 5% CO_2. The cells

were plated at 5×10^4 cells/cm^2 on glass cover slips and were allowed to attach to the coverslip for a minimum of 3 hr. Hippocampal neurons obtained from 2- to 4-day-old postnatal rats were cultured as described in Ryan and Smith (1995) and used 10 days to 3 weeks after plating. A self-built small volume electroporation device for adherent cells was used for electroporation (Teruel and Meyer, 1997). For the transfection of neurons, modified versions of the device and buffer conditions were used (Teruel et al., submitted). After transfection, the electroporation buffers were replaced with the same culture medium.

Functional Labeling of Presynaptic Terminals with FM 4-64

Functional presynaptic terminals were visualized with FM 4-64 (Molecular Probes). FM 4-64 is similar in structure and properties to FM 1-43, but its longer wavelength emission spectra make it more suitable for dual channel fluorescence microscopy in conjunction with GFP (Ziv and Smith, 1996). Cells were loaded with FM 4-64 by replacing the saline in the imaging chamber with high potassium solution (100 mM KCL, 20 mM HEPES, 1.5 mM $CaCl_2$, 30 mM NaCl, 1.5 mM $MgCl_2$ [pH 7.4], and 6 μM of FM 4-64) for 20 s and switch back to a saline solution for 5–10 min. After collecting a digital image of the labeled field (such as that in Figure 2D, left), the cells were stimulated again by switching to the same high potassium solution. The spatial distribution of the active presynaptic terminals could then be determined from a difference image (e.g., Figure 2C, center).

Diffusion Analysis

The diffusion coefficients were determined using an analysis by which a photobleached area is produced by a focused laser pulse and the fluorescence recovery is fit to sequential two-dimensional Gaussian distributions. Ratio images of the fluorescence distribution after the bleach pulse to the distribution before the pulse were used for the analysis. This analysis follows at the same time the decrease in the bleach amplitude and the increase in the bleach radius. Assuming mass conservation, the resulting fluorescence distributions were fit by:

$$F_n(x, y) = 1 - (F_o \times a_o^2/a_n^2) \times \exp(-[(x - x_o)^2 + (y - y_o)^2]/a_n^2),$$

with x and y as the pixel coordinates, a_n as the radius of the bleach diameter in the nth image, and $F_n(x, y)$ as the local relative fluorescence intensity. A least square fit routine was used to fit, at the same time, Gaussian profiles to all images in the time series. An approximate diffusion coefficient was then determined from a graph of the square of the radius, a_n^2, versus time. The diffusion coefficient can be directly obtained from the slope of this graph ($Dy/Dx = 4 \times D$; with D as the diffusion coefficient; Shen and Meyer, 1998).

Model Calculations of a Stochastic Insertion of CaMKIIβ Subunits into Heterooligomers

The probability of having one or more subunits randomly inserting into a heterooligomer is 1 − (probability of having no subunit inserted). The probability of having none inserted is $R/(R + 1)^N$, with R as the ratio of GFP–CaMKIIα to CaMKIIβ and N as the number of subunits.

Immunofluorescence

NIH-3T3 cells, RBL cells, and hippocampal neurons were cultured on glass coverslips and transfected with mRNA encoding GFP–CaMKIIβ fusion construct. Seven to eight hours after transfection, the cells were fixed for 10 min at 4°C with 4% paraformaldehyde in PBS (1.2 mM KH_2PO_4, 8.1 mM Na_2HPO_4, 138 mM NaCl, and 2.7 mM KCl [pH 7.4]). NIH-3T3 cells and RBL cells were permeabilized for 5 min at 4°C with 0.1% Triton in PBS. Hippocampal neurons were permeabilized for 10 min at 4°C with 0.1% Triton. For F-actin staining, rhodamine phalloidin (Molecular Probes) was incubated with the cells for 30 min at room temperature at a dilution of 1:300 in PBS. For the staining of postsynaptic densities, hippocampal neurons were incubated with an monoclonal PSD-95 antibody (catalog number 05–428, Upstate Biotechnology, Lake Placid, NY) overnight at 4°C at a dilution of 1:200 and then in secondary Cy3-labeled anti-mouse antibody (catalog number 115–165–062, Jackson ImmunoResearch, West Grove, PA) for 1 hr at room temperature. The cells were washed three times with PBS, and coverslips were mounted onto glass slides using buffered glycerol mounting medium.

Fibroblast Transfection and Western Blotting Assay

NIH-3T3 cells were plated in 35 mm dishes at a density of 1.0×10^5 per dish and incubated overnight at 37°C in a humid atmosphere containing 5% CO_2. Cells were transfected with 1.5–2.2 μg of pSRα–CaMKIIβ or pSRα–CaMKIIα or cotransfected with pSRα–CaMKIIβ and pSRα–CaMKIIα using lipofectin plus (GIBCO/BRL) according to manufacturer's instructions. Cells were harvested 48 hr after transfection and extracted with 10 mM Tris-HCl, 50 mM KCl, 0.1 mM EGTA, 0.1% Triton, 2 mM PMSF, and 5 μg/ml aprotinin, leupeptin, and pepstatin at room temperature for 10 min and centrifuged at 30,000 × g for 30 min at 4°C. Various fractions of the cell extract were resolved by electrophoresis on SDS-polyacrylamide gels (12%), transferred to nitrocellulose, and blotted with monoclonal anti-CaMKIIα or anti-CaMKIIβ antibody (GIBCO/BRL). The membranes were blotted using a secondary antibody conjugated to horseradish peroxidase and visualized by enhanced chemiluminescence (ECL; Amersham).

Pull-Out Protein–Protein Interaction Assay

Polyadenylated mRNA was made as described above. In many experiments, mRNA species were mixed and used for electroporation at a final concentration of typically 1 μg/μl total. The relative translation efficiency was determined by a separate in vitro translation reaction using the same mRNA as a template. Images of transfected RBL or NIH-3T3 cells were taken on a Zeiss confocal microscope 8–12 hr after electroporation. PMA (1 μM) was added and images of single cells were taken under the same configuration. Images were taken before and after PMA addition and were analyzed using NIH image software. We defined a plasma membrane translocation factor as Δ_{PM}/I_{pre} (Figure 5E).

Acknowledgments

This study was supported by National Institute of Health grants GM-48113 and GM-51457. We wish to thank Dr. Howard Schulman for the CaMKIIα and CaMKIIβ constructs, Dr. Margaret Titus for help with the biochemical fractionation assay and the F-actin binding measurements, Dr. Arturo Delozanne for insightful disscusion, and Elena Oancea for providing the Cys–GFP construct. We would also like to acknowledge the support of Wen Chen and Dr. Thomas Stauffer.

Received January 19, 1998; revised July 15, 1998.

References

Barria, A., Muller, D., Derkach, V., Griffith, L.C., and Soderling, T.R. (1997). Regulatory phosphorylation of AMPA-type glutamate receptors by CaM-KII during long-term potentiation. Science *276*, 2042–2045.

Bayer, K.U., Lohler, J., and Harbers, K. (1996). An alternative, nonkinase product of the brain-specifically expressed Ca^{2+}/calmodulin-dependent kinase II alpha isoform gene in skeletal muscle. Mol. Cell. Biol. *16*, 29–36.

Benfenati, F., Valtorta, F., Rubenstein, J.L., Gorelick, F.S., Greengard, P., and Czernik, A.J. (1992). Synaptic vesicle-associated Ca^{2+}/calmodulin-dependent protein kinase II is a binding protein for synapsin I. Nature *359*, 417–420.

Bennett, M., Erondu, N., and Kennedy, M. (1983). Purification and characterization of a calmodulin-dependent protein kinase that is highly concentrated in brain. J. Biol. Chem. *258*, 12735–12744.

Braun, A.P., and Schulman, H. (1995). The multifunctional calcium/calmodulin-dependent protein kinase: from form to function. Annu. Rev. Physiol. *57*, 417–445.

Brocke, L., Srinivasan, M., and Schulman, H. (1995). Developmental and regional expression of multifunctional Ca^{2+}/calmodulin-dependent protein kinase isoforms in rat brain. J. Neurosci. *15*, 6797–6808.

Burgin, K.E., Waxham, M.N., Rickling, S., Westgate, S.A., Mobley, W.C., and Kelly, P.T. (1990). In situ hybridization histochemistry of

Ca^{2+}/calmodulin-dependent protein kinase in developing rat brain. J. Neurosci. *10*, 1788–1798.

Caceres, A., Payne, M., Binder, L., and Steward, O. (1983). Immunocytochemical localization of actin and microtubule-associated protein MAP2 in dendritic spines. Proc. Natl. Acad. Sci. USA *80*, 1738–1742.

Chapman, P.F., Frenguelli, B.G., Smith, A., Chen, C.M., and Silva, A.J. (1995). The α-Ca^{2+}/calmodulin kinase II: a bidirectional modulator of presynaptic plasticity. Neuron *14*, 591–597.

Chen, H.J., Rojas-Soto, M., Oguni, A., and Kennedy, M.B. (1998). A synaptic Ras-GTPase activating protein (p135 SynGAP) inhibited by CaM kinase II. Neuron *20*, 895–904.

Colbran, R.J., and Soderling, T.R. (1990). Calcium/calmodulin-independent autophosphorylation sites of calcium/calmodulin-dependent protein kinase II. Studies on the effect of phosphorylation of threonine 305/306 and serine 314 on calmodulin binding using synthetic peptides. J. Biol. Chem. *265*, 11213–11219.

De Koninck, P., and Schulman, H. (1998). Sensitivity of CaM kinase II to the frequency of Ca^{2+} oscillations. Science *279*, 191–192.

Egelhoff, T.T., Brown, S.S., and Spudich, J.A. (1991). Spatial and temporal control of nonmuscle myosin localization: identification of a domain that is necessary for myosin filament disassembly in vivo. J. Cell Biol. *112*, 677–688.

Fisher, M., Kaech, S., Knutti, D., and Matus, A. (1998). Rapid actin-based plasticity in dendritic spines. Neuron *20*, 847–854.

Giese, K.P., Fedorov, N.B., Filipkowski, R.K., and Silva, A.J. (1998). Autophosphorylation of Thr^{286} of the calcium-calmodulin kinase II in LTP and learning. Science *279*, 873–876.

Glazewski, S., Chen, C.M., Silva, A., and Fox, K. (1996). Requirement for α-CaMKII in experience-dependent plasticity of the barrel cortex. Science *272*, 421–423.

Gordon, J.A., Cioffi, D., Silva, A.J., and Stryker, M.P. (1996). Deficient plasticity in the primary visual cortex of α-calcium/calmodulin-dependent protein kinase II mutant mice. Neuron *17*, 491–499.

GuptaRoy, B., and Griffith, L.C. (1996). Functional heterogeneity of alternatively spliced isoforms of *Drosophila* Ca^{2+}/calmodulin-dependent protein kinase II. J. Neurochem. *66*, 1282–1288.

Hanson, P.I., and Schulman, H. (1992). Inhibitory autophosphorylation of multifunctional Ca^{2+}/calmodulin-dependent protein kinase analyzed by site-directed mutagenesis. J. Biol. Chem. *267*, 17216–17224.

Hanson, P.I., Meyer, T., Stryer, L., and Schulman, H. (1994). Dual role of calmodulin in autophosphorylation of multifunctional CaM kinase may underlie decoding of calcium signals. Neuron *12*, 943–956.

Kanaseki, T., Ikeuchi, Y., Sugiura, H., and Yamauchi, T. (1991). Structural features of Ca^{2+}/calmodulin-dependent protein kinase II revealed by electron microscopy. J. Cell Biol. *115*, 1049–1060.

Kelly, P.T., and Vernon, P. (1985). Changes in the subcellular distribution of calmodulin-kinase II during brain development. Brain Res. *350*, 211–224.

Kelly, P.T., Shields, S., Conway, K., Yip, R., and Burgin, K. (1987). Developmental changes in calmodulin-kinase II activity at brain synaptic junctions: alterations in holoenzyme composition. J. Neurochem. *49*, 1927–1940.

Lai, Y., Nairn, A.C., and Greengard, P. (1986). Autophosphorylation reversibly regulates the Ca^{2+}/calmodulin-dependence of Ca^{2+}/calmodulin-dependent protein kinase II. Proc. Natl. Acad. Sci. USA *83*, 4253–4257.

Landis, D., and Reese, T. (1983). Cytoplasmic organization in cerebellar dendritic spines. J. Cell Biol. *97*, 1169–1178.

Llinas, R., Gruner, J.A., Sugimori, M., McGuinness, T.L., and Greengard, P. (1991). Regulation by synapsin I and Ca(2+)-calmodulin-dependent protein kinase II of the transmitter release in squid giant synapse. J. Physiol. *436*, 257–282.

Lou, L.L., Lloyd, S.J., and Schulman, H. (1986). Activation of the multifunctional Ca^{2+}/calmodulin-dependent protein kinase by autophosphorylation: ATP modulates production of an autonomous enzyme. Proc. Natl. Acad. Sci. USA *83*, 9497–9501.

Mayford, M., Wang, J., Kandel, E.R., and O'Dell, T.J. (1995). CaMKII regulates the frequency-response function of hippocampal synapses for the production of both LTD and LTP. Cell *81*, 891–904.

Mayford, M., Bach, M.E., Huang, Y.Y., Wang, L., Hawkins, R.D., and Kandel, E.R. (1996). Control of memory formation through regulated expression of a CaMKII transgene. Science *274*, 1678–1683.

McGlade-McCulloh, E., Yamamoto, H., Tan, S.E., Brickey, D.A., and Soderling, T.R. (1993). Phosphorylation and regulation of glutamate receptors by calcium/calmodulin-dependent protein kinase II. Nature *362*, 640–642.

McNeill, R.B., and Colbran, R.J. (1995). Interaction of autophosphorylated Ca^{2+}/calmodulin-dependent protein kinase II with neuronal cytoskeletal proteins. Characterization of binding to a 190-kDa postsynaptic density protein. J. Biol. Chem. *270*, 10043–10049.

Meyer, T., Hanson, P.I., Stryer, L., and Schulman, H. (1992). Calmodulin trapping by calcium-calmodulin-dependent protein kinase. Science *256*, 1199–1202.

Miller, S.G., and Kennedy, M.B. (1985). Distinct forebrain and cerebellar isozymes of type II Ca^{2+}/calmodulin-dependent protein kinase associate differently with the postsynaptic density fraction. J. Biol. Chem. *260*, 9039–9046.

Miller, S.G., and Kennedy, M.B. (1986). Regulation of brain type II Ca^{2+}/calmodulin-dependent protein kinase by autophosphorylation: a Ca^{2+}-triggered molecular switch. Cell *44*, 861–870.

Mukherji, S., and Soderling, T.R. (1994). Regulation of Ca^{2+}/calmodulin-dependent protein kinase II by inter- and intrasubunit-catalyzed autophosphorylations. J. Biol. Chem. *269*, 13744–13747.

Nicoll, R.A., and Malenka, R.C. (1995). Contrasting properties of two forms of long-term potentiation in the hippocampus. Nature *377*, 115–118.

Nomura, T., Kumatoriya, K., Yoshimura, Y., and Yamauchi T. (1997). Overexpression of alpha and beta isoforms of Ca^{2+}/calmodulin-dependent protein kinase II in neuroblastoma cells—H-7 promotes neurite outgrowth. Brain Res. *766*, 129–141.

Oancea, E., Teruel, M.N., Quest, A.F.G., and Meyer, T. (1998). GFP-tagged cysteine-rich domains from protein kinase C as fluorescent indicators for diacylglycerol signaling in living cells. J. Cell Biol. *140*, 485–498.

Omkumar, R.V., Keily, M.J., Rosenstein, A.J., Min, K.T., and Kennedy, M.B. (1996). Identification of a phosphorylation site for calcium/calmodulin-dependent protein kinase II in the NR2B subunit of N-methyl-D-aspartate receptor. J. Biol. Chem. *271*, 31670–31678.

Ryan, T.A., and Smith, S.J. (1995). Vesicle pool mobilization during action potential firing at hippocampal synapses. Neuron *14*, 983–989.

Scholz, W.K., Baitinger, C., Schulman, H., and Kelly, P.T. (1988). Developmental changes in Ca^{2+}/calmodulin-dependent protein kinase II in cultures of hippocampal pyramidal neurons and astrocytes. J. Neurosci. *8*, 1039–1051.

Schworer, C.M., Colbran, R.J., and Soderling, T.R. (1986). Reversible generation of a Ca^{2+}-independent form of Ca^{2+}(calmodulin)-dependent protein kinase II by an autophosphorylation mechanism. J. Biol. Chem. *261*, 8581–8584.

Shen, K., and Meyer, T. (1998). Identification of the minimal oligomerization domain of Ca^{2+}/calmodulin-dependent protein kinase IIa. J. Neurochem. *70*, 96–104.

Silva, A.J., Stevens, C.F., Tonegawa, S., and Wang, Y. (1992). Deficient hippocampal long-term potentiation in alpha-calcium-calmodulin kinase II mutant mice [see comments]. Science *257*, 201–206.

Soderling, T.R. (1993). Calcium/calmodulin-dependent protein kinase II: role in learning and memory. Mol. Cell. Biochem. *128*, 93–101.

Spector, I., Shochet, N.R., Blasberger, D., and Kashman, Y. (1989). Latrunculins novel marine macrolides that disrupt microfilament organization and affect cell growth. I. Comparison with cytochalasin D. Cell Motil. Cytoskeleton *13*, 127–144.

Srinivasan, M., Edman, C.F., and Schulman, H. (1994). Alternative splicing introduces a nuclear localization signal that targets multifunctional CaM kinase to the nucleus. J. Cell Biol. *126*, 839–852.

Strack, S., Choi, S., Lovinger, D.M., and Colbran, R.J. (1997). Translocation of autophosphorylated calcium/calmodulin-dependent protein kinase II to the postsynaptic density. J. Biol. Chem. *272*, 13467–13470.

Sugai, R., Takeuchi, M., Okuno, S., and Fujisawa, H. (1996). Molecular cloning of a novel protein containing the association domain of calmodulin-dependent protein kinase II. J. Biochem. *120*, 773–779.

Teruel, M.N., and Meyer, T. (1997). Electroporation induced formation of individual calcium entry sites in cell body and processes of adherent cells. Biophys. J. *73*, 1785–1796.

Vallano, M.L., Goldenring, J.R., Lasher, R.S., and Delorenzo, R.J. (1986). Association of calcium/calmodulin-dependent kinase with cytoskeletal preparations: phosphorylation of tubulin, neurofilament, and microtubule-associated proteins. Ann. NY Acad. Sci. *466*, 357–374.

Wu, G.Y., and Cline, H.T. (1998). Stabilization of dendritic arbor structure in vivo by CaMKII. Science *279*, 222–226.

Wyszynski, M., Lin, J., Rao, A., Nigh, E., Beggs, A.H., Craig, A.M., and Sheng, M. (1997). Competitive binding of α-actinin and calmodulin to the NMDA receptor. Nature *385*, 439–442.

Yamauchi, T., Ohsako, S., and Deguchi, T. (1989). Expression and characterization of calmodulin-dependent protein kinase II from cloned cDNAs in Chinese hamster ovary cells. J. Biol. Chem. *264*, 19108–19116.

Yokoe, H., and Meyer, T. (1996). Spatial dynamics of GFP-tagged proteins investigated by local fluorescence enhancement. Nature Biotech. *14*, 1252–1256.

Ziv, N.E., and Smith, S.J. (1996). Evidence for a role of dendritic filopodia in synaptogenesis and spine formation. Neuron *17*, 91–102.